Electronic Supplementary Material (ESI) for Journal of Materials Chemistry C.


# Template-free synthesis of $Na_{0.5}Bi_{2.5}Ta_2O_9/Bi_4TaO_8Cl$ nano-heterostructures via one-pot molten salt reaction for efficient photocatalysis

**Yidong Hu,** [a#] **Qingqiang Meng,** [a#] **Chunmei Li,** [b] **Yansong Zhou,** [a] **Zhonghui Han,** [a] **Weinan Xing,** [a] **Sue Hao,** [a] **and Gang Chen***[a]

[†]School of Chemistry and Chemical Engineering, Harbin Institute of Technology, No. 92 West-Da Zhi Street, Harbin 150001 (China), *Email: gchen@hit.edu.cn

[‡] Institute of Green Chemistry and Chemical Technology, School of Chemistry and Chemical Engineering, Jiangsu University, Zhenjiang 212013 (China)

# These authors contributed equally to this work

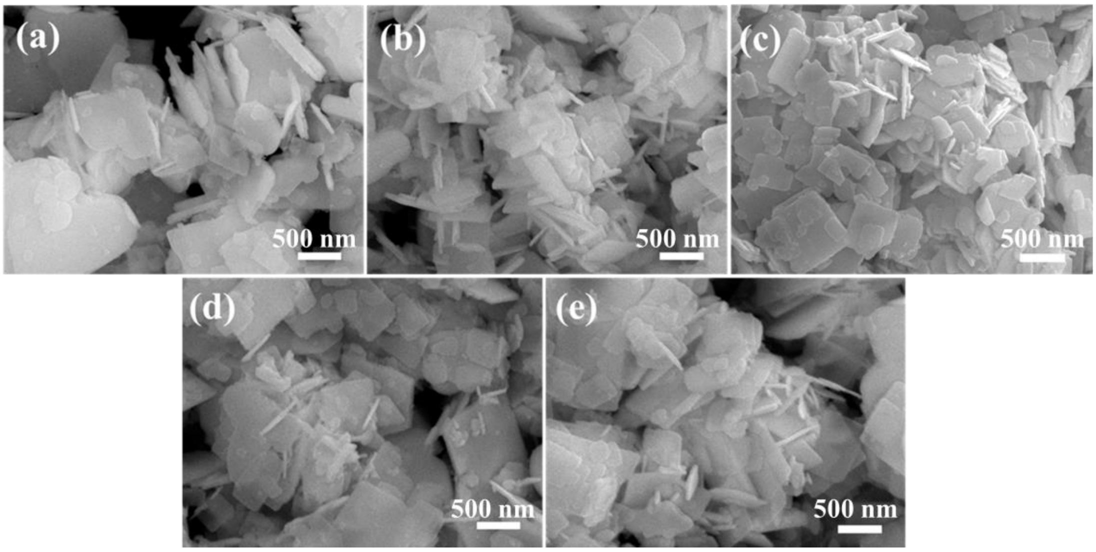


Figure S1. FESEM images of typical samples: (a) NBTO/BTOC-0, (b) NBTO/BTOC-5, (c) NBTO/BTOC-10, (d) NBTO/BTOC-15, and (e) NBTO/BTOC-20.

Table S1 BET surface areas of the typical samples

| Sample | BET surface area ($m^2$ $g^{-1}$) | Pore |
|---|---|---|
| NBTO/BTOC-0 | 4.512 | No |
| NBTO/BTOC-5 | 5.256 | No |
| NBTO/BTOC-10 | 5.808 | No |
| NBTO/BTOC-15 | 5.935 | No |
| NBTO/BTOC-20 | 6.357 | No |

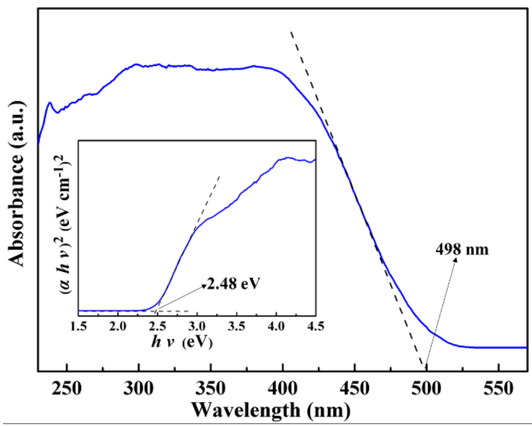


Figure S2. UV-vis DRS and corresponding Kubelka-Munk function *vs*. light energy (*hv*) curves of the BTOC catalyst (bottom left inset).

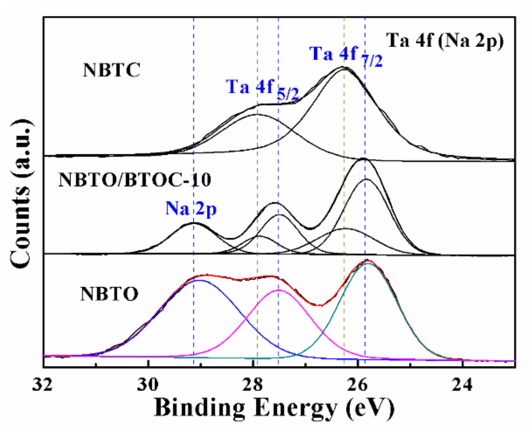


Figure S3. XPS spectra of Ta 4f for NBTO, NBTO/BTOC-10 and BTOC samples.

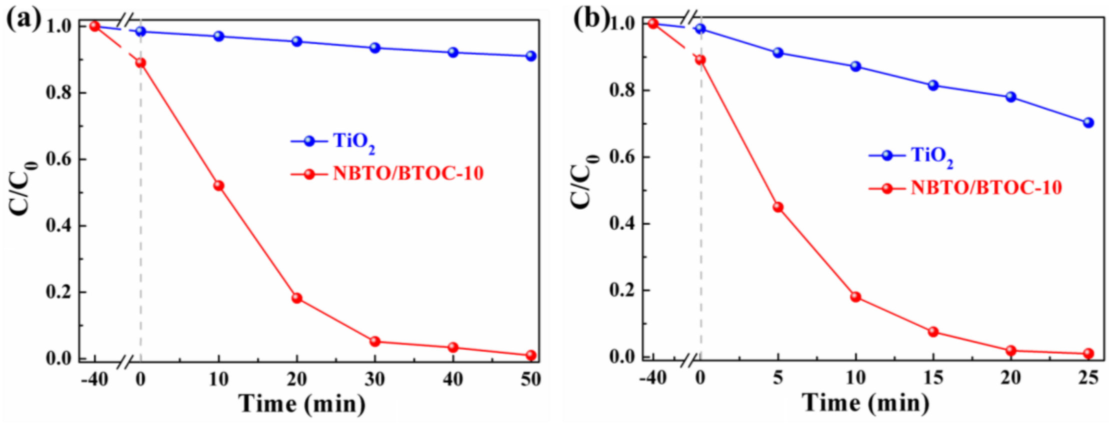


Figure S4 Dynamic curve of RhB degradation over $TiO_2$ and NBTO/BTOC-10 photocatalyst under visible-light (a) and UV-vis light (b) irradiation.

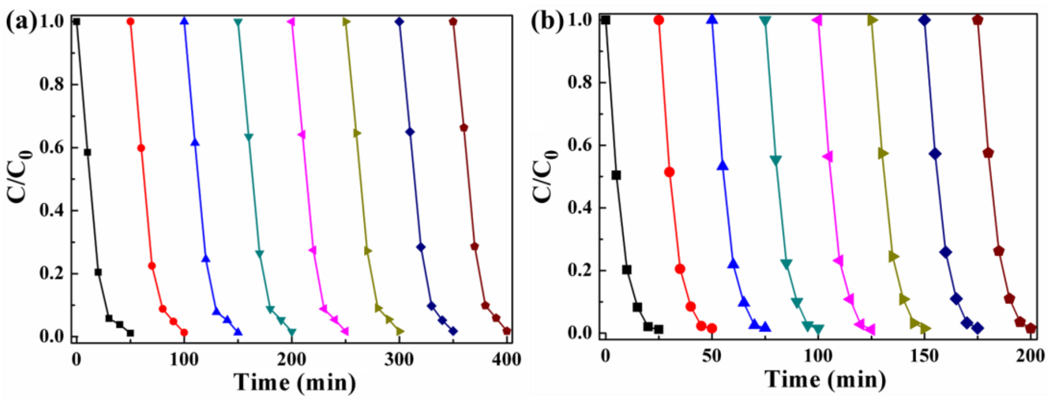


Figure S5. Photocatalytic activities of NBTO/BTOC-10 photocatalyst for the degradation of RhB under visible-light (a) and UV-vis light (b) irradiation for eight cycles.

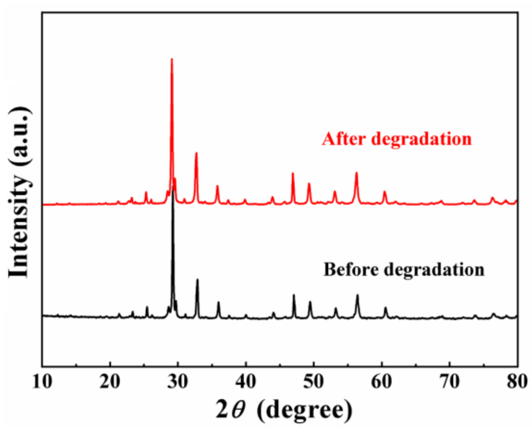


Figure S6. XRD patterns of NBTO/BTOC-10 heterostructure photocatalyst before and after RhB photocatalytic degradation under UV-vis light irradiation.

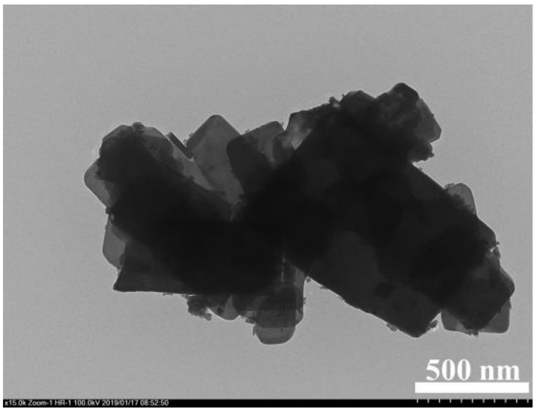


Figure S7. TEM image of NBTO/BTOC-10 heterostructure photocatalyst after RhB photocatalytic degradation under UV-vis light irradiation.

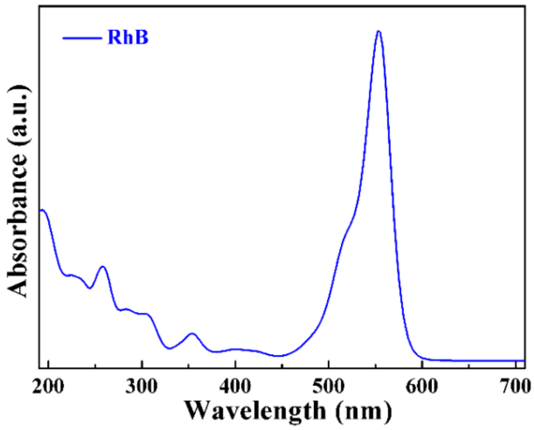


Figure S8. Absorbance spectrum of the RhB (10 mg/L).

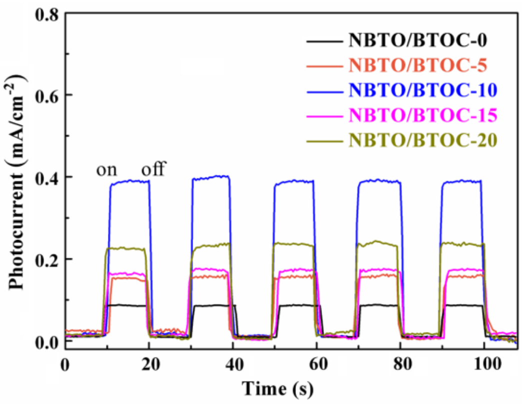


Figure S9. Comparison of transient photocurrent response of NBTO/BTOC NBTO/BTOC film electrodes under UV-vis light irradiation.

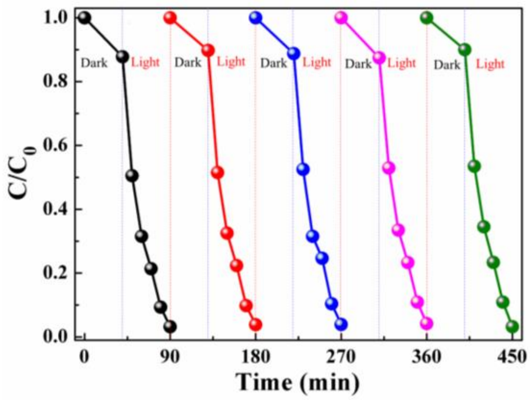


Figure S10. Photocatalytic activities of NBTO/BTOC-20 photocatalyst for the Cr (VI) reduction under visible-light irradiation for five cycles.

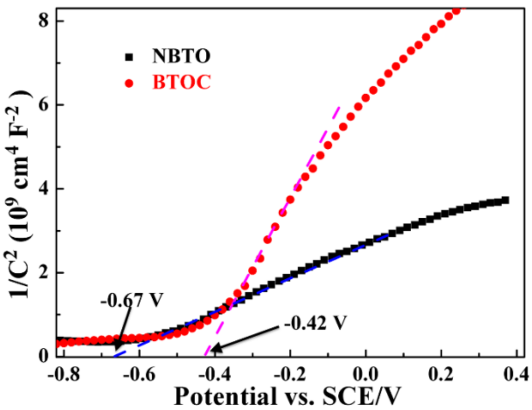


Figure S11. Mott-Schottky curves of NBTO and BTOC in 0.5 M $Na_2SO_4$ aq (Ph = 7).

The band positions of NBTO and BTOC can be calculated by the following formula:[1]

$$E_{VB} = E_{CB} + E_g$$

where $E_g$ is the band gap of the semiconductor, $E_{CB}$ is the conduction band potential, and $E_{VB}$ is the valence band potential. As shown in Figure 2b and Figure S2, the $E_g$ of NBTO and BTOC are 3.53 eV and 2.48 eV, respectively. The $E_{fb}$ potential of NBTO and BTOC determined from the Mott-Schottky plots in $Na_2SO_4$ solution (pH = 7) are −0.67 V and −0.42 V (*vs.* Ag/AgCl, Figure S5), respectively. The positive slopes indicate that both NBTO and BTOC belong to typical n-type semiconductor. For the n-type semiconductor, the position of $E_{fb}$ is approximately equal to its Fermi level.[2] It is generally recognized that the bottom of CB is about 0.1 V above the $E_{fb}$ for many n-type semiconductors.[3] A summary of the calculation results is listed in Table S2.

Table S2 $E_g$, $E_{CB}$ and $E_{VB}$ of NBTO and BTOC

| Semiconductor | $E_g$ (eV) | $E_{CB}$ (eV) | $E_{VB}$ (eV) |
|---|---|---|---|
| NBTO | 3.53 | −0.77 | 2.76 |
| BTOC | 2.48 | -0.52 | 1.96 |

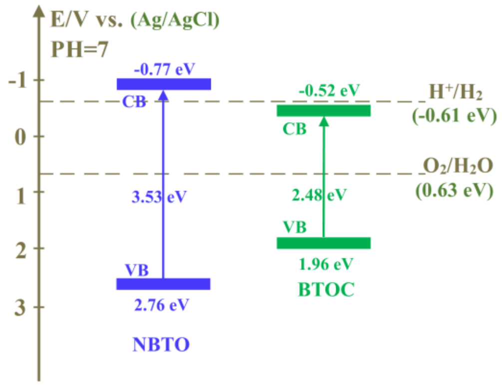


Figure S12. Schematic band structures of NBTO and BTOC.

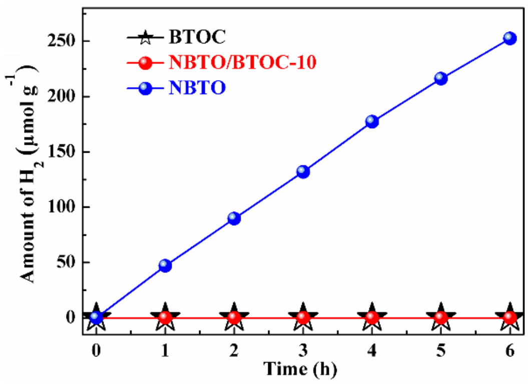


Figure S13. Comparison of photocatalytic hydrogen evolution over BTOC, NBTO, and NBTO/BTOC-10.

Based on the results of optical measurement and Mott-Schottky, a possible band alignment of NBTO/BTOC-10 is schematically illustrated in Figure S12. Both NBTO and BTOC can be easily excited by UV-vis light. Figure S11 shows the approximate band-edge positions of both NBTO and BTOC based on the above-measured flat-band potentials. The CB edge position of the NBTO

(-0.77 eV) is located above the hydrogen evolution potential and the CB edge position of the BTOC (−0.52 eV) is located below the hydrogen evolution potential at pH 7 (−0.61 eV *vs.* Ag/AgCl). As shown in Figure S13, the hydrogen generation rate of NBTO almost achieves 42 mmol $h^{-1}$ $g^{-1}$, while no $H_2$ evolution was detected with the BTOC and NBTO/BTOC-10 photocatalyst, indicating the poor reduction power of the photogenerated electrons in BTOC and NBTO/BTOC-10 photocatalysts when comparing with that of NBTO photocatalyst. Therefore, Since NBTO has a more negative CB level and more positive VB level than BTOC does, photogenerated electrons are transferred from the CB of NBTO to BTOC, meanwhile, the holes in NBTO will migrate to the VB of BTOC in NBTO/BTOC-10 nanocomposites.

## References


1 M. A. Butler and D. S. Ginley, *J. Electrochem. Soc.*, 1978, **125**, 228–232.

2 K. Azumi, T. Ohtsuka and N. Sato, *J. Electrochem. Soc.*, 1987, **134**, 1352–1357.

3 A. Ishikawa, T. Takata, J. N. Kondo, M. Hara, H. Kobayashi and K. Domen, *J. Am. Chem. Soc.*, 2002, **124**, 13547–13553.